Chapter 12

Numerical Simulation of Fiber Laser Operated in Passively Q-Switched and Mode-Locked Regimes

Sorin Miclos, Dan Savastru, Roxana Savastru and Ion Lancranjan

Additional information is available at the end of the chapter

http://dx.doi.org/10.5772/61882

Abstract

The aim of this chapter is to highlight the role of simulation methods as tools for analysis of low and medium average power fiber laser operated in passively Q-switched and/or mode-locking regimes into the design of various applications such as materials microprocessing of sensor applications. The chapter's purpose consists in making available to specialists in the field of lasers, electro-optics and even nano-photonics improved procedures for designing high-accuracy remote sensors dedicated to large range of laboratory, industrial and military applications. The reason that this chapter deals with passive optical Q-switching and mode-locking techniques tailored for fiber lasers is the high percentage of sensing devices operating in this regime. Numerical simulation results obtained for this class of laser emitters can be used for other types of lasers, such as optical fiber lasers. There are briefly presented the two main mathematical methods used to analyze solid laser oscillators in passive optical Q-switching regime: the coupled rate equations approach and the iterative approach. The validation of the presented numerical simulation methods is done by comparison with experimental results.

Keywords: Fiber laser, all-fiber passive optical Q-switching, all-fiber mode-locking numerical simulation

1. Introduction

Erbium, ytterbium and ytterbium/erbium co-doped fiber lasers operated in mode-locking regime (ML) are an extremely useful tool for an increasing number of researches, medical and industrial applications. Their main characteristic is their output consisting of a phase coherent train of very short pulses, less than a picosecond. The application range of ML-operated fiber lasers spans from micro-machining metals [1] all the way to the most precise frequency measurements ever made [2]. Based on the many proposals for new technologies that utilize

mode-locked lasers [3, 4], it is clear that these lasers will be an invaluable tool for future technologies.

Here, we present simulation results obtained in analyzing a particular type of mode-locked fiber laser, namely those using erbium (Er), ytterbium (Yb) or ytterbium/erbium-doped or co-doped single-mode (SM) optic fiber as active medium and/or saturable absorber [5-13]. These types of lasers are intensively investigated because of their advantages, i.e. low cost, low power consumption, long term of use, robustness, and ease of long-distance transmission (through single-mode fiber). The performed analysis is pointing to a special topic of such lasers, namely the stabilization of the repetition frequency of these lasers. Initial demonstrations of these lasers showed large amounts of high frequency noise in these systems [14, 15]. We then turned our attention towards investigation of reduction of frequency noise in these systems for design improvement, synchronizing remotely located fiber lasers using this fast actuator in conjunction with a stabilized fiber link.

The performed simulation of Er, Yb or Yb/Er fiber lasers operated in ML regime has the scope of developing a software toolbox dedicated to an optimal laser design for micromachining glass and bare SM optic fiber.

2. Theory

The ML technique is based on phase locking many different frequency modes of a laser cavity. For practical reasons, as their bulk solid state counterparts fiber lasers are used in many applications which require high peak power and pulse energy [16-23]. There are two most well-established techniques for pulsing fiber lasers: Q-switching and mode locking in either active or passive form [17, 19-21]. Because of its "in principia" simplicity, one of the most used device for pulsing fiber lasers is the passive Q-switch cell manufactured, in essence, of a saturable absorber material. Q-switching is an effective method to obtain giant short pulses from a laser by spoiling the cavity loss periodically with a modulator inside the resonator cavity [17, 19]. In this technique, the pump delivers constant power all time, where the energy is stored as accumulated population inversion during the OFF times (high loss). During the ON time, the losses are reduced and the accumulated population difference is released as intense pulse of light. Q-Switching allows the generation of pulses of mJ energy, ns duration and few Hz to hundreds of kHz repetition rate [17-21]. For shorter pulses in picoseconds or sub-picoseconds ranges, mode- locking is the main mechanism [21-23]. The phase locking of different frequency modes of a fiber laser cavity imposes the laser to produce a continuous train of extremely short pulses rather than a continuous wave (CW) of light [16-18]. In principle, a continuous train of extremely short pulses can be generated from a passively Q-switched laser. It is also possible that the laser generates a continuous train of extremely short pulses which have amplitude modulated by the saturable absorber and having an envelope of the laser pulses peaks similar to Q-switched pulses [21-23]. The difference between these two scenarios of fiber laser emission obtained under continuous pumping of doped optic fiber active media lies in the optical phase of the pulses. The mode-locked pulses are phase-coherent

http://dx.doi.org/10.5772/61882

with each other, while the Q-switched pulses are not [24-26]. This simple fact has massive consequences regarding the application of these two types of lasers. This technique induces a fixed phase relationship between the longitudinal modes of the laser cavity. Interference between these modes causes the laser light to produce a train of pulses. Locking of mode phases enables a periodic variation in the laser output which is stable over time, and with periodicity given by the round trip time of the cavity [27-33].

To understand the mode-locking process, even if it appears too basic, it is useful to begin by investigating a CW pumped fiber laser, which is supposed to have a CW output in the frequency domain. For a single longitudinal mode CW laser, considered as having a Fabry-Perot cavity and a frequency defined as

$$\nu = \frac{c}{2nL} \tag{1}$$

it can be considered that one resonant mode of the laser cavity overlaps in frequency with the gain medium. Thus, this hypothetical fiber laser emits a CW beam with a narrow range of frequencies defined as

$$E(t) = E_1 \exp\left[i\left(\omega_1 t + \varphi_1\right)\right] \tag{2}$$

In general, however, the gain medium could overlap with several modes. We can describe the output of such a laser in the time domain as

$$E(t) = \sum_{1}^{N} E_n \exp\left[i\left(\omega_n t + \varphi_n\right)\right] \tag{3}$$

where the sum is over all of the lasing cavity modes, E_n is the amplitude of the nth mode, ω_n is the angular frequency of the nth mode, and ϕ_n is the phase of the nth mode. For the single-mode laser, this sum just has one term as given above. As we will see, the phase term plays the key role in the difference between incoherent multimode lasing and mode locking. It can be considered an increasing range of overlap between the gain bandwidth and with fiber laser cavity modes. In this case, there are N terms in Equation (3). The output of such a laser depends critically if there is a well-defined phase relationship between the N modes. If each mode has a randomly varying phase with respect to the other modes, then a time domain detector on the output would show us that the laser is emitting a CW beam with a large amount of intensity noise, while a frequency domain detector would show us that the energy was contained in narrow spikes (with lots of intensity noise) spaced evenly by the free spectral range (FSR) of the cavity. However, if we can fix the relative phases to a clearly defined value, then the situation changes dramatically. With fixed phase relationships, the N modes can combine to

interfere in such a way as to constructively interfere at multiples of the roundtrip time of the cavity, while they destructively interfere elsewhere. This process creates shorter pulses as the number of phase-locked modes increases [27-33].

An obvious question to be asked concerns how this well-defined relation between fiber laser cavity longitudinal modes is exactly obtained, implicitly how the phase locking of the longitudinal modes is obtained. The answer to this question could be obtained from the time domain picture of mode-locking. It is clearly experimentally established that a mode-locked laser produces ultra-short pulses at a rate equal to the round trip time of the optical cavity. The explanation of this experimental observation is that there has to be some part of the fiber laser that allows the pulse emission over CW radiation. This statement equates to say that there is needed of some element providing high loss at low intensity (CW radiation) and lower loss at high intensity (pulsed operation). Such a device is a saturable absorber. The operational principles of atoms or molecules as saturable absorbers are straightforward: low-intensity light is absorbed by the atoms and re-emitted into 4π steradians (i.e. out of the laser cavity), while high-intensity light fully excites the atoms and passes most of its photons through the medium. The main feature of the saturable absorber is its decreasing loss with increasing intensity. As is seen immediately, this behavior can be mimicked with optical processes that have nothing to do with actual atomic or molecular resonance absorption.

It is interesting to note that the history of mode-locked lasers began not long after the first demonstration of a continuous wave lasing in 1960, and it is intimately connected with search for obtaining substances having a saturable absorption. Maiman's [34] ruby laser was created at Hughes Research Laboratory in California; the creation of the first mode-locked laser would occur at Bell Laboratories in New Jersey. In 1964, Hargrove et al. [35] used an extremely clever acousto-optic technique to provide a loss modulation in a helium-neon laser cavity, which led to the laser being actively mode locked. In 1965, Mocker and Collins showed that they could achieve transient locking of the modes of a multimode Q-switched laser using a saturable Q-switching dye (cryptocyanine in methanol) [17]. Since only a few modes were involved in this process, the pulse widths were on the order of tens of nanoseconds. Their technique, however, required no active modulator, and thus was the first demonstration of passive mode locking. The drawback of this dye was that it required the laser to be Q-switched in order to saturate and thus the laser emitted mode-locked pulses only at the Q-switched intervals. The transient nature of the mode locked pulses proved to be problematic in practical applications (ultrafast spectroscopy, nonlinear optics, etc.). This problem was solved in 1972 when Ippen et al. introduced a laser based on the saturable dye (Rhodamine 6G) that could mode lock continuously [18]. The pulses from this laser were found to have pulse widths of only 1.5 picoseconds. After this demonstration, many researcher efforts were done in order to push the gain bandwidth further with other types of saturable absorbers, including, in the first stages, different types of dyes, and after that period, solid-state saturable absorbers such as the ones made of semiconductor materials (SESAM) and of crystals or glasses doped with different types of ions such as Co^{2+}, Cr^{4+}, Zn^{2+} and others. In the case of fiber laser, one newly appearing mode-locking technique consists of using optic fiber doped with Sm or Tm ions or even with the same type of ions as the optic fiber active medium.

http://dx.doi.org/10.5772/61882

Regarding the ML operation of fiber laser, it is worth to analyze with a type of saturable absorber known as an effective saturable absorber. It is a special class of saturable absorbers, using processes other than atomic/molecular absorption. These saturable absorbers do not have to rely only on actual atomic transitions. This means that the recovery time for the saturable absorber can be much faster than for atomic transitions. Slow saturable absorbers can produce pulses with duration less than a picosecond by shortening the leading edge of the pulse via saturable absorption and the trailing edge via gain saturation. However, if the atomic transition of saturable absorber recovers fast enough, it can shorten both sides of the pulse using the saturable absorber effect which is achieved by exploiting the intensity- dependent index of refraction defined as

$$n(I) = n_0 + n_2 I \tag{4}$$

where n_0 is the index of refraction, n_2 is the nonlinear index coefficient and I is the optical intensity. The recovery time for a saturable absorber based on this effect is essentially instantaneous because non-resonant optical processes are extremely fast inducing a nonlinear index to respond on the order of a few optical cycles. Two types of mode locking based on effective saturable absorbers are mostly used and reported in literature: Kerr lens mode locking (KLM) and additive pulse mode locking (APM).

KLM is based on lens creation into the gain medium as an effect of the nonlinear index of refraction, lens which causes self-focusing of the beam [36, 37]. KLM is combined with an intracavity aperture, this effect creates a situation where the cavity prefers pulsed operation because if the laser is in CW operation, there is a high loss due to the aperture, while in pulsed operation the beam focuses through the aperture with minimal loss.

APM is realized by interference of circulating pulses. In the first realization of APM [38, 39], this interference was between pulses propagating in two coupled cavities. The main cavity has the gain medium and an output coupler, while the secondary cavity has a nonlinear section, an optical fiber. Pulses that are coupled to the nonlinear cavity experience an intensity-dependent phase shift. When these pulses are coupled back to the main cavity they can be made to overlap with the normal pulses in such a way as to constructively interfere at their peaks, while destructively interfering at their wings. Thus, the addition of multiple pulses results in pulse shortening on every round trip, just like a real saturable absorber. One special type of APM is based on nonlinear polarization rotation (P-APM) [39] and is particularly useful in a fiber laser cavity. The basic idea is that the added pulses are not from separate cavities, but are co-propagating with different polarization. Elliptically polarized pulses propagate in a Kerr medium to produce nonlinear polarization rotation. Experimentally, this situation can be produced by inserting a quarter-wave plate into the fiber cavity, so that linear polarization can be turned into elliptical. The highest intensity part of the pulse (i.e. the peak) undergoes a nonlinear phase shift and thus rotates its polarization some amount. The wings of this pulse, which have low intensity, do not undergo this phase shift and thus experience no rotation. A quarter-wave plate and linear polarizer at the output of the Kerr medium (fiber) turn the

intensity-dependent polarization into an intensity-dependent transmission. This type of mode locking can produce pulse widths that are close to the gain bandwidth limit of Er (≈100 fs) [39].

Mode-locked Er or Yb/Er fiber lasers have many advantages to be considered regarding various applications. One main advantage consists in the fact that an all fiber cavity needs no realignment. Also, the components needed to build a mode-locked all fiber laser are relatively cheap due to their mass production in the telecommunications industry. As an example, a nonlinear polarization mode-locked all fiber laser could be built for an expense of less than 4, 000 USD. For comparison, a typical solid-state titanium doped sapphire mode-locked laser could be purchased from a vendor for around 100, 000 USD. While the typical output power of a Ti:Sapphire system is roughly an order of magnitude larger than that of a mode-locked Er fiber laser, it is straightforward and inexpensive to build an Er amplifier that allows the Er-based system to reach average power levels close to those of the mode locked Ti:Sapphire oscillator. Using a frequency doubling crystal, one can even transform the 1, 550 nm centered Er laser to Ti:Sapphire wavelengths around 750 nm. Finally, the relatively small gain bandwidth of the Er gain medium can easily be converted into an octave of spectrum using highly nonlinear fiber. All of these factors have played a part in the rapid emergence of fiber lasers in the world of ultrafast physics in the past 10 years. Erbium-doped fiber is particularly useful over other rare-earth doped fibers (i.e. ytterbium, neodymium, thulium, etc.) due to silica glass's low loss window in the telecommunications C band (conventional band: 1, 530–1, 565 nm).

In order to obtain a better understanding of the operation of an Er or Yb/Er-doped mode-locked fiber laser, the rate equation approach is useful. This approach starts with the Yb and Er ions energy level diagrams, schematically presented in Figure 1. The Er ion is a quasi-3 level system, meaning that although the lowest state in the lasing scheme is not the true ground state, it is still low energy enough that it has some population due to thermal excitation.

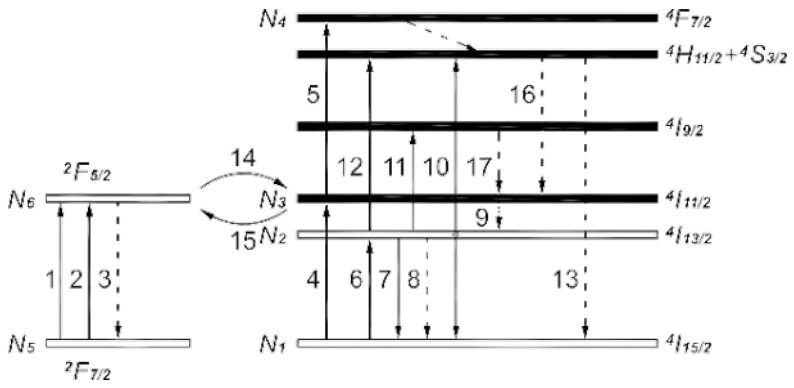

Figure 1. The Yb and Er active ions energy levels diagrams.

The pumping of Er ions is accomplished by either 980 nm or 1, 450 nm light generated by a semiconductor diode laser. In Figure 2, an example of mode-locked Er or Yb/Er-doped all-fiber

http://dx.doi.org/10.5772/61882

laser is presented. Here, pumping diodes are laser pumping diodes with CW or pulsed-chopped emission at 976 nm at powers up to 25 W, combiner and WDM are coupling the pump power into a double clad Yb-doped fiber used as active medium, Yb-DCF is Yb-doped double clad fiber active medium with 15 μm diameter core and 15 m length, HR-FBG is a high reflectivity (99 %) FBG used as rear laser mirror and OC-FBG is a low reflectivity (15 %) FBG used as laser output coupler.

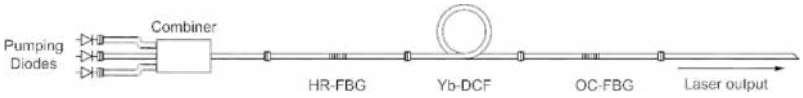

Figure 2. Configuration diagram of passively Q-switched all-fiber laser using an "excess" of fiber.

Regarding the pumping efficiency using 980 nm diode laser radiation, Yb/Er co-doped has better performances in comparison with simple Er-doped fiber laser. The role of Yb ions is the one of absorbing the pump radiation at 975-980 nm and due to its intense fluorescence at wavelength 980 nm, a wavelength closed to Er ions absorption band, to transfer optical excitation to Er ions. For single Er-doped optic fiber active medium, the 980 nm and the 1, 450 nm schemes result in similar efficiencies.

The trivalent erbium ion, when pumped with 980 nm light, is excited to the $^4I_{11/2}$ state, which decays to $^4I_{13/2}$ (see Figure 1). The decay between $^4I_{11/2}$ and $^4I_{13/2}$ is non-radiative (multiple phonon decay) and occurs within a few μs, while the metastable state ($^4I_{13/2}$) has a lifetime of about 10 ms. Since the $^4I_{11/2}$ state has such a short lifetime, we can make the approximation that this highest excited state has zero steady-state population (i.e. no population accumulates). This approximation reduces the number of participating energy levels to two. We can now write down the relevant rate equations that describe the number of erbium ions in the upper (N_2) and lower (N_1) energy levels

$$\frac{dN_1(t)}{dt} = A_{21}N_2(t) + \left(N_2(t)\sigma_e^s - N_1(t)\sigma_e^s\right)\frac{I_s}{h\nu_s} + \left(N_2(t)\sigma_e^p - N_1(t)\sigma_a^p\right)\frac{I_p}{h\nu_p} \tag{5}$$

$$\frac{dN_2(t)}{dt} = -A_{21}N_2(t) + \left(N_1(t)\sigma_a^s - N_2(t)\sigma_e^s\right)\frac{I_s}{h\nu_s} + \left(N_1(t)\sigma_a^p - N_2(t)\sigma_e^p\right)\frac{I_p}{h\nu_p} \tag{6}$$

where A_{21} is the Einstein A coefficient (inverse lifetime) for spontaneous emission, σ_a^s is the cross section for stimulated absorption at the signal wavelength, σ_a^s is the cross section for stimulated emission at the signal wavelength, σ_a^p is the cross section for stimulated absorption at the pump wavelength, σ_a^p is the cross section for stimulated emission at the pump wavelength, I_s is the signal intensity, I_p is the pump intensity, $h\nu_s$ is the energy of each individual

signal photon and $h\nu_p$ is the energy of each individual pump photon. By dividing the beam intensity by the photon energy of that beam, we get the total number of photons passing through a given area (i.e. photon flux).

To achieve lasing, we must have population inversion such that $N_2 > N_1$. The threshold for this condition occurs when the ion density in N_2 just equals N_1. By setting the Equations (5) and (6) equal and solving for the pump intensity, we find the threshold intensity for population inversion

$$I_{pth} = \frac{h \cdot \nu_p}{\tau\left(\sigma_a^p - \sigma_e^p\right)} \tag{7}$$

For a pump wavelength of 980 nm, this intensity is roughly 6 kW/cm^2. Since the mode field area of a single-mode Er fiber is around 20 μm^2, the pump power needed to achieve inversion is on the order of a few mW. This calculation is for a lossless cavity, however. Due to losses in fiber splices, the output coupler and losses in the coupling of the pump diode to the fiber, the actual pump power required for lasing threshold is of the order of tens of mW (typical 980 nm pump diodes reach average powers beyond 600 mW). It is also instructive to look at the evolution of the signal beam as it propagates through the gain (amplifying) section of the laser cavity. A simple differential equation governs the signal in the presence of a 2-level gain medium

$$\frac{dI_s(z)}{dz} = \left(N_2(t) \cdot \sigma_e^s - N_1(t) \cdot \sigma_a^s\right) \cdot I_s(z) \tag{8}$$

with the solution

$$I_s(z) = I_0 \exp(gl) \tag{9}$$

$$I_s(z) = I_0 \exp\left[\left(N_2(t) \cdot \sigma_e^s - N_1(t) \cdot \sigma_a^s\right) \cdot l\right] \tag{10}$$

where I_0 is the intensity entering the gain section, l is the total length of the gain section and g is the gain defined as

$$g(t) = \left(N_2(t) \cdot \sigma_e^s - N_1(t) \cdot \sigma_a^s\right) \tag{11}$$

For our analysis, we will consider the absorption of the signal beam to be zero, thus

http://dx.doi.org/10.5772/61882

$$g(t) = N_2(t) \cdot \sigma_e^s \tag{12}$$

The gain is then dependent only on the density of excited atoms N_2 and the emission cross section of the excited Er atoms at the signal wavelength σ_a^s. The emission cross section is a constant, thus to determine the gain we only have to find N_2. Using Equation (8), we have

$$\frac{dN_2(t)}{dt} = -A_{21}N_2(t) + \left(-N_2(t)\sigma_e^s\right)\frac{I_s}{h\nu_s} + \left(N_1(t)\sigma_a^p\right)\frac{I_p}{h\nu_p} \tag{13}$$

In the small signal limit, the pump intensity is much larger than the signal intensity ($I_p >> I_s$). Using this approximation along with the fact that we are analyzing a steady-state scenario (d/d$t \rightarrow 0$), we can ignore the I_s term and set the left-hand side of Equation (13) equal to zero. Solving for N_2 yields

$$N_2(t)\left(I_s << I_p\right) = \left(N_1(t)\sigma_a^p\right)\frac{I_p}{A_{21}h\nu_p} \tag{14}$$

$$N_2(t)\left(I_s << I_p\right) = \tau\left(N_1(t)\sigma_a^p\right)\frac{I_p}{h\nu_p} \tag{15}$$

$$N_2(t)\left(I_s << I_p\right) = \tau R \tag{16}$$

where τ is the lifetime of the excited state, defined as

$$\tau = \frac{1}{A_{21}} \tag{17}$$

and R is excitation rate which is defined as

$$R = \left(N_1(t)\sigma_a^p\right)\frac{I_p}{h\nu_p} \tag{18}$$

This equation shows that the density of excited atoms in the small-signal limit is simply given by the lifetime of the exited state (τ) multiplied by excitation rate R. Using the fact that g is defined as

$$g(t) = N_2(t) \cdot \sigma_e^s \tag{19}$$

the small signal gain is g_0 is defined by the relation

$$g_0(t) = \tau \cdot N_2(t) \cdot \sigma_e^s \cdot R \tag{20}$$

As the signal beam is increased to higher intensity, however, we must take into account the term in Equation (13) that involves I_s. Solving for N_2 yields

$$N_2(t) = \frac{N_2(I_s << I_p)}{1 + \frac{I_s}{I_{sat}}} \tag{21}$$

And the large signal gain is thus

$$g(t) = \frac{g_0}{1 + \frac{I_s}{I_{sat}}} \tag{22}$$

where I_{sat} is the saturation intensity defined as

$$I_{sat} = \frac{1}{\sigma_e^s \tau} \tag{23}$$

And finally, the differential change in signal intensity per length of gain in the strong pump regime is

$$\frac{dI_s(z)}{dz} = \frac{I_s \cdot g_0}{1 + \frac{I_s}{I_{sat}}} \tag{24}$$

The picture of the signal evolution is now complete. At low signal levels, there is an exponential increase in the number of signal photons in the gain medium. However, as the signal level is increased further, the gain begins to saturate and asymptotically approaches a value defined by

$$g(t) \approx I_{sat} \cdot g_0 = R \tag{25}$$

http://dx.doi.org/10.5772/61882

Thus, as expected, at high signal levels, the signal intensity increases linearly with the pump intensity. The fundamental characteristics of lasing, namely, the small-signal gain and the gain saturation have now been covered.

It is worth to mention an important aspect related to the mode-locking theory, namely, the frequency comb. With the advent of the frequency comb [40] in the late 1990s, mode-locked lasers, including the fiber ones, began to receive much attention concerning the frequency metrology applications. The frequency comb appears as a simultaneous solution for two important purposes separated by a vast gap to be achieved using mode-locking laser, especially fiber lasers. These two purposes are: on one side, the field of precision measurements imposes creation of actuated lasers that would have the narrowest possible spectral linewidth and, on the other side, the field of ultrafast spectroscopy was mainly interested in creating extremely short time domain bursts of electric field, which necessarily require that the pulses have a large spectral bandwidth. These two goals, which seem to be in direct opposition of each other, can be achieved simultaneously with a frequency comb.

As was mentioned, the frequency comb is based on mode-locked lasers [40-42]. In fact, mode-locking and frequency comb are definitions used interchangeably. This is not quite right, however, since technically a frequency comb really refers to a mode-locked laser that has been carrier-envelope phase stabilized. The frequency comb can be understood by using and by combining its description in time and frequency domains [40-42]. The time domain output of the laser can be viewed as the multiplication of the fast electric field oscillations and an envelope function, representing a modulation of electric field amplitude by the envelope function. The ultimate limit on the width of this envelope would be an envelope that encompasses only 1 cycle of the electric field, in other words, corresponding to one round trip along laser cavity. It can be shown that the envelope travels at a speed known as the group velocity v_g defined as

$$v_g = \frac{c}{n - \lambda \frac{dn}{d\lambda}} \tag{26}$$

while the electric field fast oscillations travel at the phase velocity v_p defined as

$$v_p = \frac{c}{n} \tag{27}$$

These two velocities are, in general, not equal and thus lead to a walk-off or slippage between the two entities, known as carrier-envelope offset phase. Using the shift theorem of Fourier transforms [42], we see that the Fourier transform turns this time domain phase slip into a frequency offset, f_0. Thus, the optical frequencies of the comb can be defined in terms of two frequencies as

$$\nu_n = n \cdot f_{rep} + f_0 \tag{28}$$

where ν_n is the optical frequency of the nth comb mode and f_{rep} is the repetition frequency of the laser, which is related to the optical length of its cavity. Clearly, a random variation of the offset frequency would smear out the comb in frequency space and make it useless for any sort of precision measurement. An analogy to this sort of measurement would be like trying to measure the length of something with a ruler that is always moving back and forth slightly. Thus, it is clear that to do any sort of precision measurement with a mode-locked laser, we need to stabilize this offset frequency (and thereby produce a frequency comb).

The first technique that achieved the ability to measure (and thus stabilize) f_0 relied on the so-called *f*-2*f* interferometer, a complicated experimental setup which is quite a technical achievement by itself. This technique is based on a simple manipulation of Equation (28). In this scheme, light from a Ti:sapphire laser was sent through a highly nonlinear fiber with low net dispersion to broaden the bandwidth of the pulses to an octave [40]. The octave spanning pulses were then coupled into an interferometer where in one arm the light was passed through a second harmonic crystal and underwent sum-frequency-generation (SFG). The two beams were then recombined on a beam-splitter, sent through an optical filter, and detected onto a photodetector to produce a heterodyne beat at f_0. The octave spanning pulse bandwidth ensures that we have optical frequencies present in a range from ν_n to ν_{2n}, while the second harmonic arm converts the ν_n light to ν_{2n} light via SFG. Filtering out the highest frequencies with the optical filter, and using the frequency comb equation, we can thus write the frequencies present in the two arms as

$$\nu_{2n} = 2n \cdot f_{rep} + 2\nu_n \cdot f_0 = 2n \cdot f_{rep} + 2f_0 \tag{29}$$

Once these two beams form a heterodyne beat on the photodetector, we can take the difference frequency which is

$$2\nu_n - \nu_{2n} = \left(2n \cdot f_{rep} + 2f_0\right) - \left(2n \cdot f_{rep} + f_0\right) = f \tag{30}$$

The first demonstration of this method [40] opened the door for experiments involving the frequency comb. Precision metrology benefited dramatically from the compact all-in-one nature of the frequency comb, while new techniques such as broadband cavity-ring down spectroscopy [43-44] have been developed based on the comb.

Another theoretical issue of mode-locked fiber laser concerns the consequence of nonlinear effects produced in the optic fiber during ultrashort light pulses propagation. It can be noticed that Equations (5–25) describe what should be defined as the energetic part of the mode-locked ultrashort laser propagation phenomena. In Equations (5–25), the cycle pump absorption –

http://dx.doi.org/10.5772/61882

population inversion – light energy at the laser wavelength is analyzed. Equations (26–29) are helpful for defining the aspects related to the repetition frequency of ultrashort light pulses. It is to be observed that because of the fiber optic guiding effect, the ultrashort light pulses propagation, even with energies on the nJ scale and full width half measure time duration of ps or fs is happening through core transverse area, meaning extremely large light intensity. Due to the square variation law of light intensity versus its electric field amplitude, it can be concluded that nonlinear effects can be produced. Quantitatively, all these qualitative comments can be developed starting from the system of Maxwell equations describing electromagnetic pulses propagation through optic fibers. In the system of Maxwell equations, the polarization vector of the dielectric propagation medium can be split into two terms, one linear and the other corresponding to its nonlinear variation.

$$\frac{\partial A}{\partial z} + \beta_1 \frac{\partial A}{\partial t} + \frac{i}{2}\beta_2 \frac{\partial^2 A}{\partial t^2} = i\gamma \left|A\right|^2 A \tag{31}$$

where A represents the propagating electromagnetic field potential, the β_1-term is responsible for the group velocity (with the transformation $T=t-\beta_1 z$ which transforms to the moving frame of the pulse), β_2 is often called the group-velocity dispersion (GVD) parameter. This equation is an example of the nonlinear Schrödinger equation (NLSE).

3. Simulation Results

As previously mentioned, the simulation of the Er- or Yb/Er-doped all-fiber laser was performed aiming to the development of a set of toolbox useful for evaluation of passively Q-switched and/or mode-locked laser dedicated to glass and optic fiber micro-processing. For accomplishing this task, sense previous experience in this field constitutes an advantage [45-47]. The simulation scripts can be grouped into two sets: the first one developed on the bases of Equations (1-3) and describing the parameters of a ML fiber laser at the first level and the second, the more complex one, using Equations (5-22) which treats the propagation of ultrashort laser pulses through laser resonator. The second set is an attempt to solve nonlinear Schroedinger equation.

In Figures 3, 4, 5 and 6 are presented results obtained in investigation of the noise factor role in definition of mode-locked laser pulses emitted by an Yb/Er fiber laser as schematically presented in Figure 2, using the simulation codes of the first set. A CW pump power of 55 W was considered. The simulated mode-locked Yb/Er laser is composed of a double clad fiber having a length in excess (9 m). The value of noise factor, d, is increased from zero up to 1.5. Figures 3 to 6 represented the overlapping between gain bandwidth and fiber laser resonator modes. In Figure 3 d is considered as zero and the mode-locked laser pulses are clearly defined.

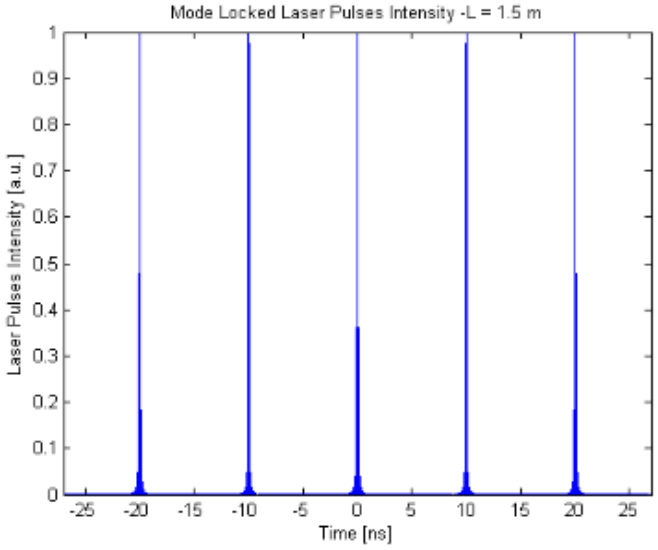

Figure 3. Laser pulse intensity versus time simulated for an Yb/Er fiber laser with 9 m length, "excess" of fiber, considering a noise factor $d = 0$.

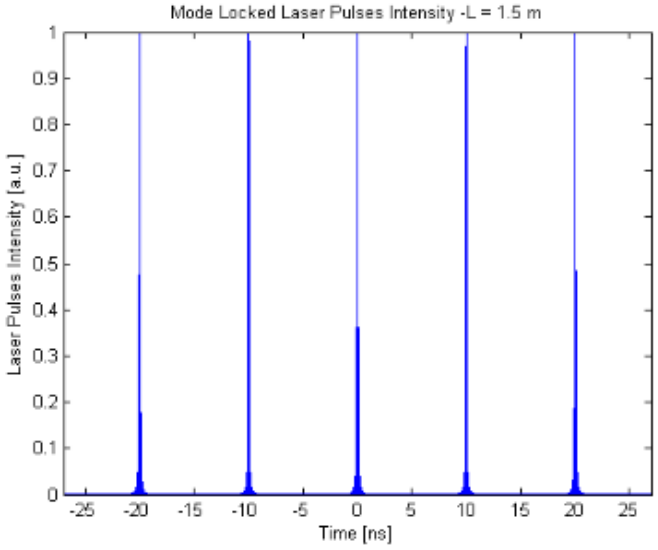

Figure 4. Laser pulse intensity versus time simulated for an Yb/Er fiber laser with 9 m length, "excess" of fiber, considering a noise factor $d = 0.05$.

http://dx.doi.org/10.5772/61882

In Figure 4, a small increase of d value, up to 0.05 was considered and some noise appearing on the wings of the mode-locked pulses can be observed. In Figure 5, the d factor has a value of 0.5 and the noise on the wings of mode-locked pulses is more evident. In Figure 6, the noise factor is increased up to 1.5 and its effects on the wings of mode-locked pulses are visible. This process creates shorter pulses as the number of phase-locked modes increases.

In Figures 7, 8 and 9, the simulation results are obtained using the second set of codes in the case of the same previously defined mode-locked Yb/Er all-fiber laser. In Figure 7, as can be observed, the mode-locked laser pulses are presented as analyzed in time domain. In Figure 8 results of the same analysis obtained in defining the fiber laser pulse spectrum are presented considering frequency as input are presented. In Figure 9, the simulated pulse spectrum is presented but considering wavelength as the argument.

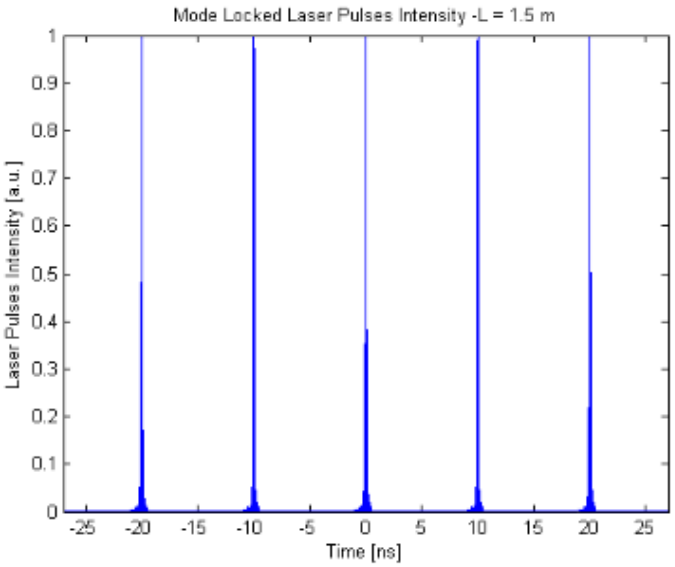

Figure 5. Laser pulse intensity versus time simulated for an Yb/Er fiber laser with 9 m length, "excess" of fiber, considering a noise factor $d = 0.5$.

In each Figure (7 to 9), the simulation was performed for three moments: t_0 – the initial moment, $t_0 + 40\ t_r$ and $t_0 + 80\ t_r$, where t_r is the laser cavity round trip time.

Simulations of the propagation equation (nonlinear Schrödinger equation) presented in Figures 7, 8 and 9 are helpful for the understanding of pulse propagation in optical fibers. Especially chromatic dispersion, nonlinear effects and their interplay, leading to physical phenomena like solitons, can be investigated with these simulations. The possibility to take a characterized pulse and to let it propagate through various fibers (as long as the fiber parameters are known) is helpful for the understanding of the pulse compression after the amplifier.

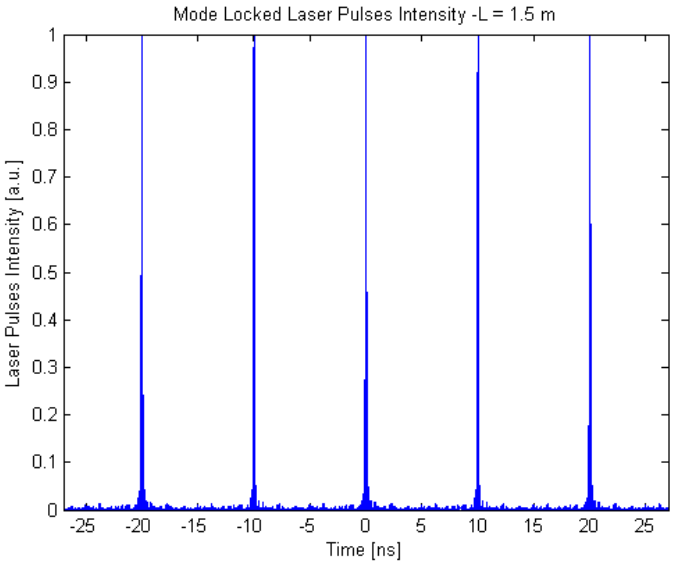

Figure 6. Laser pulse intensity versus time simulated for an Yb/Er fiber laser with 9 m length, "excess" of fiber, considering a noise factor $d = 1.5$.

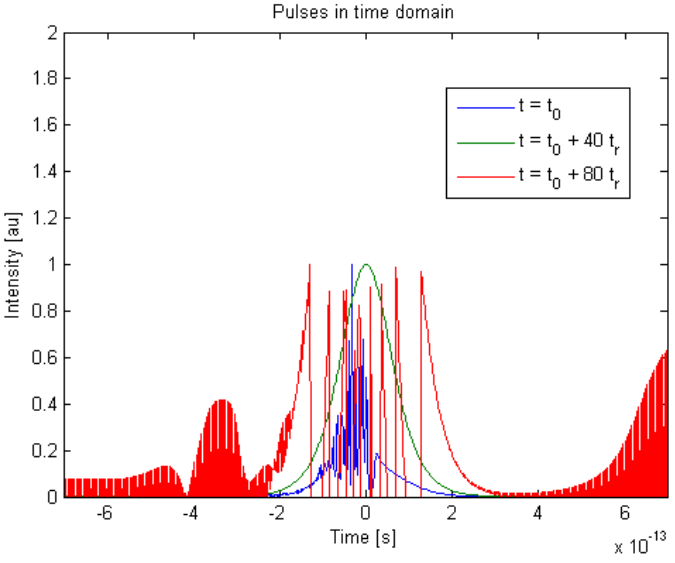

Figure 7. Laser pulse intensity analyzed in time domain in the case of an Yb/Er fiber laser with 9 m length, "excess" of fiber.

http://dx.doi.org/10.5772/61882

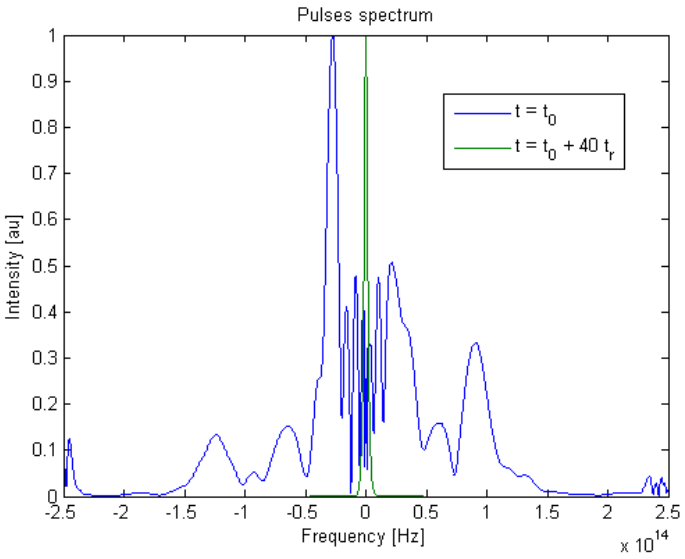

Figure 8. Laser pulse spectrum simulated for an Yb/Er fiber laser with 9 m length, "excess" of fiber, considering frequency as input.

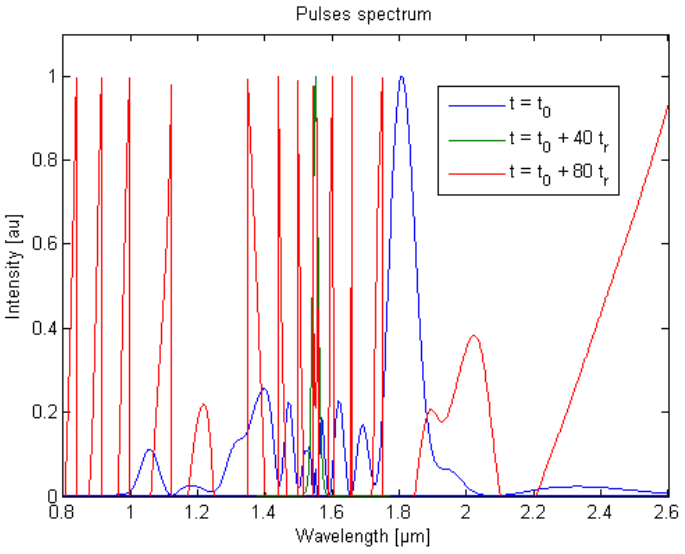

Figure 9. Laser pulse spectrum simulated for an Yb/Er fiber laser with 9 m length, "excess" of fiber, considering wavelength as input.

The simulation also made it possible to investigate the spectral broadening of an ultrashort laser pulse in a highly nonlinear fiber. The results show that it is theoretically possible to create an octave spanning supercontinuum with the pulse from our laser system. The simulation makes possible the design of a measuring system for the carrier-envelope frequency based on a *f*-2*f* interferometer. It is possible to investigate the spectrum that barely spans a factor of two into an attempt to detect a carrier-envelope set frequency beat above the noise.

The performed simulation has as a future objective, the construction of mode-locked Er all-fiber laser using a special technique, the polarization additive-pulse mode locking (P-APM) procedure. It is based on the fact that due to the nonlinear refraction of the optic fiber, different intensities see a different index of refraction. For elliptically polarized radiation, the net result is polarization rotation. The investigated P-APM mechanism works like this: a pulse with a strongly elliptic polarization is sent into a Kerr-medium; dependent on the intensity there will be more or less polarization rotation; combined with a polarizer which only transmits the rotated part (higher intensity), this acts as a "pulse-shortener". The mode-locking elements are located in the free-space path of the fiber laser. The polarizer is represented by a polarizing beam-cube and a Faraday-isolator or by an optic fiber polarization controller. The quarter-wave plate (QWP) right, or the optic fiber which have this function, makes the polarization elliptical; the other two wave plates change the polarization to maximize the transmission at pulsed operation. It can be noticed that the mode-locking is self-starting, meaning that the pulse builds up from initial CW fluctuations, just as it is the case of an excess Er fiber laser (see Figure 2) and is analyzed in Equations (1-3).

4. Conclusions

The main purpose of this chapter is to present a possible development of simulation codes applicable for Er or Yb/Er all-fiber lasers operated in mode-locking regime with glass and fiber optic micro-machining application. In this sense, the basic theoretical notions are defined in Section 2: Theory and examples of simulation codes use could be observed in Section 3: Simulation Results. A fairly good agreement between the simulated data and the similar ones reported in literature can be noticed.

Author details

Sorin Miclos*, Dan Savastru, Roxana Savastru and Ion Lancranjan

*Address all correspondence to: miclos@inoe.ro

National Institute R&D of Optoelectronics - INOE , Magurele, Ilfov, Romania

http://dx.doi.org/10.5772/61882

References

[1] Ostendorf A, Kamlage G, Chichkov B. Precise deep drilling of metals by femtosecond laser pulses. RIKEN Review: Focused on Laser Precision Microfabrication. 2003;50:87-9.

[2] Osky W, et al. Single-atom optical clock with high accuracy. Phys Rev Lett 2006;97:020801.

[3] Ye J. Absolute measurement of a long, arbitrary distance to less than an optical fringe. Opt Lett 2004;29:1153-5.

[4] Schibli T. Combs for dark energy. Nat Photonics 2008;2:712-3.

[5] Tsai T-Y. et al. All-fiber passively Q-switched erbium laser using mismatch of mode field areas and a saturable-amplifier pump switch. Opt Lett 2009;34:2891-3.

[6] Wu B, Chu PL. Fast optical switching in Sm^{3+}-doped fiber. IEEE Phot Technol Lett 1996;8:230-2.

[7] Fotiadi AA, et al. All-fiber passively Q-switched Ytterbium laser. Proc CLEO/Europe 29B, CJ2-3, 2005.

[8] Tsai T-Y, et al. Saturable absorber Q-and gain-switched all-Yb^{3+} all-fiber laser at 976 and 1064 nm. Opt. Expr 2010;18: 23523-8.

[9] Moore S W et al. 400 μJ 79 ns amplified pulses from a Q-switched fiber laser using an Yb^{3+}-doped fiber saturable absorber. Opt. Expr 2012;20:23778-9.

[10] Soh DBS, Bisson SE, et al. () High-power all-fiber passively Q-switched laser using a doped fiber as a saturable absorber: numerical simulations. Opt. Lett 2011;36:2536-8.

[11] Fotiadi AA, et al. () Dynamics of All-Fiber Self-Q-switched Ytterbium/Samarium Laser. Proc CLEO/QELS/PhAST 15, CMC4, 2007.

[12] Fotiadi AA, et al. All-fiber coherent combining of Er-doped amplifiers via refractive index control in Yb-doped fibers by two-wavelengths optical signal. Proc CLEO/Europe, CJ3-5, 2009.

[13] Huang JY, et al. High-power 10-GHz self-mode-locked Nd:LuVO4 laser. Appl Opt 2008;47:2297-302.

[14] Hong F, Minoshima K, Onae A, et al. Broad-spectrum frequency comb generation and carrier-envelope offset frequency measurement by second-harmonic generation of a mode-locked fiber laser. Opt Lett 2003;28:1516-8.

[15] Hudson DD, Holman KW, et al. Mode-locked fiber laser frequency-controlled with an intracavity electro-optic modulator. Opt Lett 2005;30:2948-50.

[16] Hargrove LE, Fork RL, Pollack MA. Locking of HeNe laser modes induced by synchronous intracavity modulation. Appl Phys Lett 1964;5:4-5.

[17] Mocker HW, Collins RJ. Mode competition and self-locking effects in a Q-switched ruby laser. Appl Phys Lett 1965;7:270-3.

[18] Ippen EP, Shank CV. Dienes A, Passive mode locking of the CW dye laser. Appl Phys Lett 1972;21:348-50.

[19] Rüdiger P. Encyclopedia of Laser Physics and Technology, 1ed. John Wiley & Sons, 2008.

[20] Digonnet MJF. Rare-earth-doped fiber lasers and amplifiers, 2d ed. Marcel Dekker, 2001, vol. 25.

[21] Svelto O, Hanna DC. Principles of Lasers. Springer, 1998.

[22] Saleh BEA, Teich MC, Masters BR. Fundamentals of Photonics, Second Edition. John Wiley & Sons, 1991.

[23] Wang Y, Xu C-Q. () Actively Q-switched fiber lasers: Switching dynamics and nonlinear processes. Prog Quantum Electronics. 2007;31:131-216.

[24] Schreiber T, Nielsen CK, et al. Microjoule-level all-polarization-maintaining femtosecond fiber source. Opt Lett 2006;31:574-6.

[25] Seung BC, Song H, Gee S, Dug YK. Self-starting passive mode-locked ytterbium fiber laser with variable pulse width. Proc. SPIE - Fiber Lasers VII: Technology, Systems, and Applications. 2010;7580:75802C.

[26] Ortac B, Plotner M, et al. Experimental and numerical study of pulse dynamics in positive net-cavity dispersion mode locked Yb-doped fiber lasers. Optics Exp 2007;15:15595-602.

[27] Jang GH, Yoon TH. Environmentally-Stable All-normal-dispersion Picosecond Yb-doped Fiber Laser with an Achromatic Quarter-wave-plate. Laser Phys 2010;20:1463-8.

[28] Lian FQ, Fan ZW, et al. Ytterbium doped all-fiber-path all-normal dispersion mode-locked laser based on semiconductor saturable mirror. Laser Phys 2011;21:1103-7.

[29] Turchinovich D, Liu X, Laegsgaard J. () Monolithic all-PM femtosecond Yb-fiber laser stabilized with a narrow-band fiber Bragg grating and pulse-compressed in a hollow-core photonic crystal fiber. Optics Express. 2008;16:14004-14.

[30] Tian X, Tang M, et al. High-energy wave-breaking-free pulse from all-fiber mode-locked laser system. Optics Exp 2009;17:7222-7.

[31] Song R, Chen H, et al. A SESAM passively mode-locked fiber laser with a long cavity including a band pass filter. J Optics. 2011;13:035201.

http://dx.doi.org/10.5772/61882

[32] Liu J, Xu J, Wang P. High Repetition-Rate Narrow Bandwidth SESAM Mode-Locked Yb-Doped Fiber Lasers. IEEE Photonics Technol Lett 2012;24:539-41.

[33] Prochnow O, Ruehl A, et al. All-fiber similariton laser at 1 μm without dispersion compensation. Optics Exp 2007;15:6889-93.

[34] Maiman TH. Stimulated optical radiation in ruby. Nature. 1960;187:493-4.

[35] Hargrove LE, Fork RL, Pollack MA. Locking of HeNe laser modes induced by synchronous intracavity modulation. Appl Phys Lett 1964;5:4-5.

[36] Spence DE, Kean PN, Sibbett W. 60-fsec pulse generation from a self-mode-locked Ti:sapphire laser. Opt Lett 1991;16:42-4.

[37] Ell R, et al. Generation of 5-fs pulses and octave-spanning spectra directly from a Ti:sapphire laser. Opt Lett 2001;26:373-5.

[38] Mollenauer LF, Stolen RH. The soliton laser. Opt Lett 1984;9:13-5.

[39] Stolen RH. Nonlinearity in fiber transmission. Proc IEEE 1980;68:1232-6.

[40] Jones DJ, Diddams SA, et al. Carrier-envelope phase control of femtosecond mode-locked lasers and direct optical frequency synthesis. Science. 2000;288:635-40.

[41] Cundiff S, Ye J, Hall J. Optical frequency synthesis based on mode-locked lasers. Rev Sci Instrum 2001;72:3749-59.

[42] Walker R, Udem T, et al. Frequency dependence of the fixed point in a fluctuating frequency comb. Appl Phys B 2007;89:535-43.

[43] Cundiff S, Ye J. Colloquium: Femtosecond optical frequency combs. Rev Mod Phys 2003;75:325-32.

[44] Everson KM, Wells JS, et al. Accurate frequencies of molecular transitions used in laser stabilization: the 3.39-μm transition in CH4 and the 9.33- and 10.18-μm transitions in CO_2. Appl Phys Lett 1973;22:192-9.

[45] Lancranjan I, Miclos S, Savastru D. Numerical simulation of a DFB-fiber laser sensor (I). J Opt Adv Mat 2010;12:1636-45.

[46] Lancranjan II, Savastru D, et al. Analysis of a passively q-switched Nd:YAG slab laser oscillator/amplifier system. Proc SPIE 2012;8547:854712.

[47] Savastru D, Vlase A, et al. Numerical simulation of laser techniques for art conservation – Part I – Fiber laser analysis. UPB Sci Bull-Ser. A 2011;73:167-78.